Russian Journal of General Chemistry, Vol. 71, No. 5, 2001, pp. 742–751. Translated from Zhurnal Obshchei Khimii, Vol. 71, No. 5, 2001, pp. 791–801.

Quantum-Chemical Calculation of the Mechanism of Gas-Phase Hydrolysis of Benzenesulfonyl Chloride

V. V. Kislov and S. N. Ivanov

Ivanovo State University, Ivanovo, Russia

Received August 9, 1999

Abstract—The potential energy surface of gas-phase hydrolysis of benzenesulfonyl chloride was calculated by PM3 quantum-chemical method. The structural and energy parameters were calculated for all the intermediates and transition states; activation parameters and the thermodynamic functions of the reaction were determined. The axial orientation of the nucleophilic attack is preferred when the reactive center is attacked by the water molecule occurring at the axis of the C–S bond from the sulfonyl group. Gas-phase hydrolysis of benzenesulfonyl chloride is an exothermic process involving formation of an unstable five-coordinate intermediate. The calculated apparent rate constants and activation parameters of the process are compared with the published data on hydrolysis of benzenesulfonyl chloride in water and aqueous-organic solvents.

Large body of experimental data has been accumulated to date on the kinetics of hydrolysis of arylsulfonyl halides $ArSO_2Hlg$ **I** in water [1, 2], aqueous-organic solvents [3–6], and sulfuric acid [7], as well as hydrolysis of thiophenesulfonyl halides [8]. Diverse concepts explaining the hydrolysis mechanism of these compounds were summarized in reviews [9–11]. At the same time, theoretical calculations for the mechanisms of the nucleophilic substitution reactions at the sulfur atom of the sulfonyl group have not been reported as yet, despite the fact that the S_N2 processes at saturated [12–14] and carbonyl [15] carbon atoms have been studied fairly extensively, both in the gas phase and with the solvent effects taken into account. Nucleophilic processes involving the sulfonyl reactive center in compounds **I** exhibit a number of features making these reactions of enhanced interest. These are, above all, participation of the 3*d* orbitals of the sulfur atom in bonding (sp^3d^2 hybridization), the hypervalent character of the sulfur atoms, and the tetracoordination of the reactive center.

This work continues our systematic quantum-chemical and experimental investigations of the structure and reactivity of compounds **I** [16–18]. We conducted semiempirical PM3 calculations of the potential energy surface for the gas-phase hydrolysis of benzenesulfonyl chloride **II**. This enabled identification of the possible intermediates and transition states for this reaction and, hence, the most probable mechanism of the elementary chemical stage at the sulfonyl reactive center.

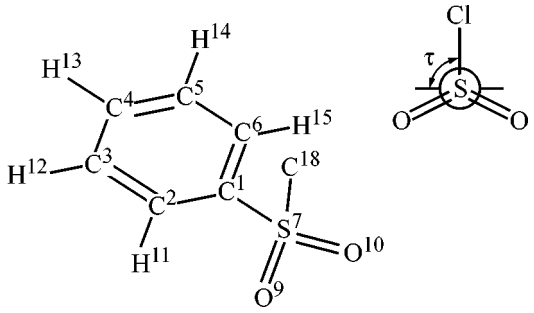

It is known that the reaction mechanism can be revealed by calculating the potential energy surface and subsequently localizing the stationary points on it, namely, the minima and the first-odrer saddle points corresponding to the initial states, transition states, and intermediates in the process [12, 19, 20]. In view of the fact that calculations of the total potential energy surface for all the $3N - 6$ independent variables are practically impossible even for medium-sized systems, we restricted ourselves in this work to calculations of "truncated" two- and three-dimensional surfaces for which we varied one or two internal coordinates of the system that changed most profoundly in the course of the reaction. By analyzing the calculated surfaces or contour maps (sections), we localized the stationary points and then carried out the geometry optimization for the corresponding structures.

The calculations utilized the PM3 semiempirical method [21] in the restricted Hartree–Fock approximation with the MOPAC 6 package [22]. We showed previously [16, 17] that, compared to MNDO and

1070-3632/01/7105-0742 $25.00

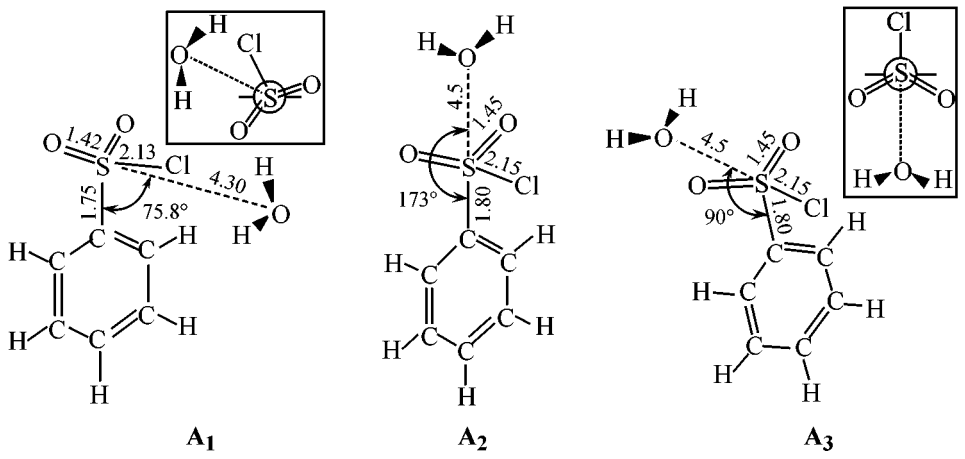

Fig. 1. Different types of the nucleophilic attack in hydrolysis of benzenesulfonyl chloride: (**A**$_1$) frontal, (**A**$_2$) axial, and (**A**$_3$) rear.

AM1 methods, PM3 affords more precise calculations of the structural parameters (close in precision to *ab initio* calculations in extended bases) and of the heats of formation of compounds **I**, as well as of other sulfonyl derivatives. Also, the potentialities of the PM3 method for calculations of the systems involving hydrogen bonds [23] afford easy simulation of the solvent effect in the supramolecule approximation. The geometry optimization was performed without symmetry type restrictions, using the Eigenvector Following optimization method at the rms gradient norm of 0.001. For each point of the potential energy surface we optimized all the internal coordinates of the system, except for the surface coordinates chosen. The two-dimensional potential curves were calculated at a step of 0.005 Å (2000–3000 points on the average), and three-dimensional surfaces, with over 5000 points. The geometry optimization for the transition states involved calculations of the Hesse matrix for each cycle. After the geometry optimization we checked the type of the stationary point, namely, calculated the vibrational spectrum and checked the occurrence in the spectrum of the unique negative vibrational frequency. In calculations of the thermodynamic parameters for the intermediate states, the negative frequency was excluded from the calculation of the statistical sums for vibrational movement.

Calculations of the S_N2 reaction mechanisms should take into account various lines of the nucleophilic attack at the reactive center and their corresponding reaction routes [12]. In the case of the simplest gas-phase reactions of substitution at the saturated carbon atom ($X^- + CH_3Y$) there can be two stereochemically different lines of the attack, frontal and rear. As shown by theoretical and experimental investigations, the rear attack involving the configuration inversion is preferable. It was found that the gas-phase mechanism of these reactions is described by a two-well potential curve whose minima correspond to the pre-reaction ($X^- \cdot CH_3Y$) and post-reaction ($XCH_3 \cdot Y^-$) complexes with a strongly asymmetric structure and localized charge. These complexes are formed in the gas phase only (in solutions, the mechanism is described by the potential curve typical for S_N2 reactions, namely, that with the unique transition state) and have an electrostatic nature; the estimated stabilization energy for the complexes ranges from –10 to –20 kcal mol^{-1} [12].

In the case of hydrolysis of compounds **I**, the axial attack should also be taken into consideration, along with the frontal and rear attacks. In the axial attack, the oxygen atom of the attacking water molecule lies on the C^1–S^7 bond axis. As both the nucleophile and the substrate are neutral species, stable pre-reaction complexes, by contrast to the substitution at the saturated carbon atom, can hardly be formed in the gas phase. As shown in [18], in calculations for aqueous clusters of molecules of **II**, the stabilization energy of the H complexes of **II** with one water molecule does not exceed –15 kJ mol^{-1}. This suggests that the elementary stage in hydrolysis should be realized via direct collision of the benzenesulfonyl chloride and water molecules.

Figure 1 presents the initial states **A**$_1$, **A**$_2$, and **A**$_3$ for the frontal, axial, and rear attacks, respectively. Preliminary calculations showed that the frontal attack does not require fixing any coordinates of the system, as whatever the initial orientation of the water molecule in the vicinity of the sulfo group, the subsequent optimization always results in insertion of the nucleophile between the chlorine and oxygen atoms from

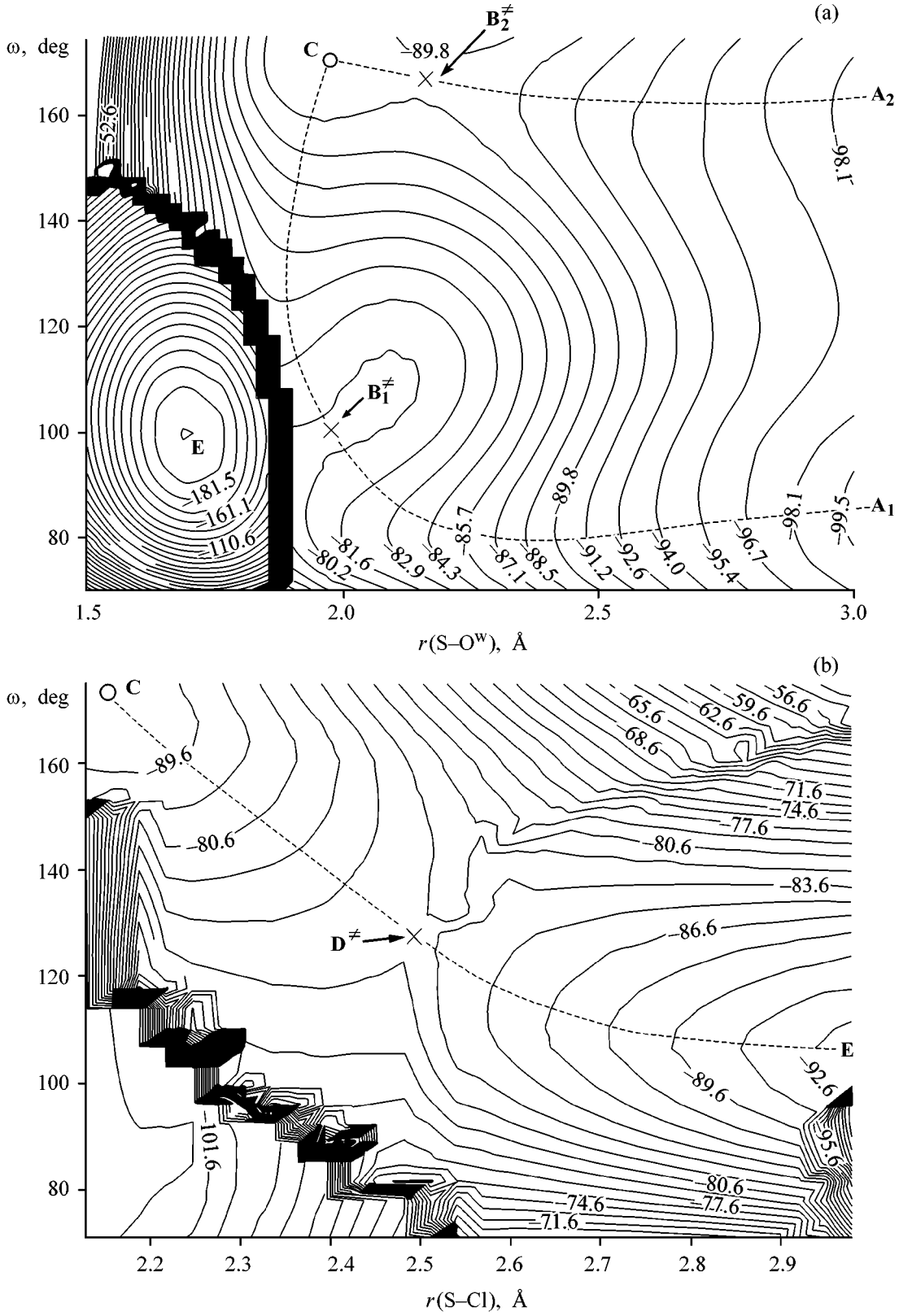

Fig. 2. Two-dimensional contour maps of the potential energy surface of benzenesulfonyl chloride hydrolysis for the stages of (a) formation of intermediate **C** and (b) conversion of **C** to the reaction products; the numbers in the isolines correspond to the heats of formation of the levels, kJ mol^{-1}.

the sulfonyl group. The calculations for the axial attack require freezing of the ω($C^1S^7O^w$) bond angle (atoms from the attacking water molecule are indexed with "w") at close to 180°. In the case of the rear attack, it is necessary to fix the torsion angle $O^wS^7C^1C^2$, that is, the angle of rotation of the S^7–O^w bond about the benzene ring plane, at 90°C.

The calculations of the potential curves $\Delta H^0_{f,298} = f[r(S^7–O^w)]$ for various lines of the nucleophilic attack showed that the reaction coordinate method has little to offer for investigating the mechanism of benzenesulfonyl chloride hydrolysis, as the curves being calculated (especially in the case of the frontal attack) have discontinuities. In the vicinity of the points corresponding to the transition states the reaction pathway being calculated becomes discontinuous and does not pass through the point corresponding to the transition state, which is due to ambiguous choice of the reaction coordinate [19, 20]. The pathway of the reaction under study is not unambiguously determined by the S^7–O^w distance, as moving of the reaction system along the process coordinate also involves significant changes in other internal coordinates of the system, in particular, in the bond angle ω. For this reason, we calculated the three-dimensional potential energy surface in the coordinates S^7–O^w distance and angle ω. Figure 2a presents the two-dimensional contour map of the calculated surface which suggests two reaction routes. The first route corresponds to the frontal attack and passes through the $\mathbf{B_1^{\neq}}$ transition state (its optimized structure is shown in Fig. 3a). The second route corresponds to the axial attack and passes through the $\mathbf{B_2^{\neq}}$ transition state (Fig. 3b). By both routes the system comes to a local minimum corresponding to the intermediate complex **C** in the reaction pathway. The optimized structure of this imtermediate is shown in Fig. 3c.

The calculated potential energy surface shown in Fig. 2a enabled elucidation of the structure of the transition states only for the intermediate **C** formation stage, because of the discontinuities of the surface at the $r(S^7–O^w)$ values under 1.9 Å. The reason is that the S^7–Cl^8 distance sharply increases (elimination of the chlorine atom) with minor changes in $r(S^7–O^w)$. Identification of the transition state for the second stage of the hydrolysis involving conversion of the intemediate **C** into the reaction products requires calculation of the potential energy surface in the coordinates of distance S^7–Cl^8 and angle ω. The continuity of the potential energy surface in all the reaction pathway sections can, most probably, be achieved only in the case of a four-dimensional surface. This means that it should be defined by the internal coordinates of the system: the S^7–O^w and S^7–Cl^8 bond lengths and the bond angle ω. Figure 2b presents the contour map for the potential energy surface of the reaction for the stage at which the intermediate complex **C** is converted to the reaction products, state **E**. This map enables clear localization of the saddle point with its corresponding transition state $\mathbf{D^{\neq}}$ in the second stage of hydrolysis. The optimized structure for $\mathbf{D^{\neq}}$ is shown in Fig. 3d, and the structure of the final state of the reaction **E**, in Fig. 3e.

Figure 4a shows the calculated potential curve $\Delta H^0_{f,298} = f[r(S^7–O^w)]$ for the rear location of the water molecule (Fig. 1c). The calculation showed that the rear attack yields another intermediate complex, $\mathbf{C_1}$, whose structure is shown in Fig. 3f. The optimized structure of the transition state $\mathbf{B_3^{\neq}}$ for this process is shown in Fig. 3g. As seen from Fig. 4a, with further decrease in $r(S^7–O^w)$ the intermediate $\mathbf{C_1}$ does not convert to the reaction products. This is evidenced by permanent increase in the heat of formation of the system at $r(S^7–O^w) < 1.9$ Å. This is quite understandable in view of the fact that the $\mathbf{C_1} \rightarrow \mathbf{E}$ conversion requires inversion of the configuration and elimination of the charged particle $Cl^–$. This process should be extremely unfavorable energetically in the gas phase. In the case of the frontal and axial attacks the water molecule occurs in the vicinity of the chlorine atom, which makes possible elimination of the Cl and H^w atoms in the form of a neutral HCl molecule. A second route can be assumed by which the intermediate $\mathbf{C_1}$ will convert to the reaction products. In this case, $\mathbf{C_1}$ will first convert to the complex **C**, which requires an increase in ω from 91° to 180°. To check the possibility of such a route, we performed calculations for a fragment of the potential energy surface in the $r(S^7–O^w)$ and ω coordinates for the rear location of the water molecule. The calculated surface is shown in Fig. 4b; it is seen that the surface does not contain saddle point corresponding to the $\mathbf{C_1} \rightarrow \mathbf{C}$ process. From the local minimum point $\mathbf{C_1}$ the system will move along a more favorable path, i.e., return to the initial state of the reaction via the transition state $\mathbf{B_3^{\neq}}$. These results suggest that in the gas phase the rear attack will not convert the system to the reaction products, i.e., this hydrolysis route is not realized. It can be assumed that in a polar medium, where the $Cl^–$ anion being eliminated gets solvated by the solvent molecules, the reaction can involve direct conversion of the intermediate $\mathbf{C_1}$ to the reaction products.

The calculations of the potential energy surface suggest the existence of two routes for gas-phase hydrolysis of **II** by which the system converts from

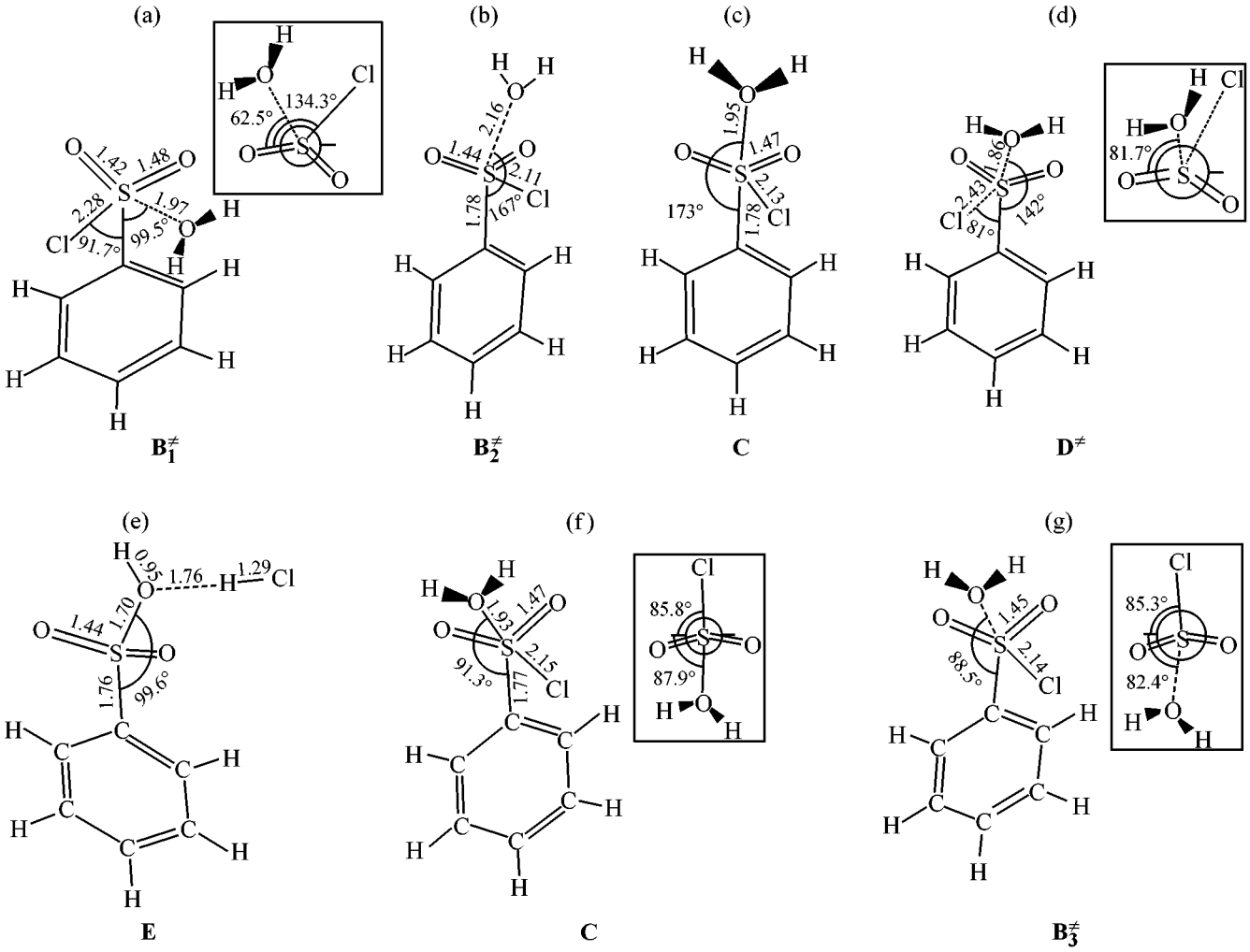

Fig. 3. Optimized structures of (a, b, d, g) transition states, (c, f) intermediates, and (e) product of benzenesulfonyl chloride hydrolysis.

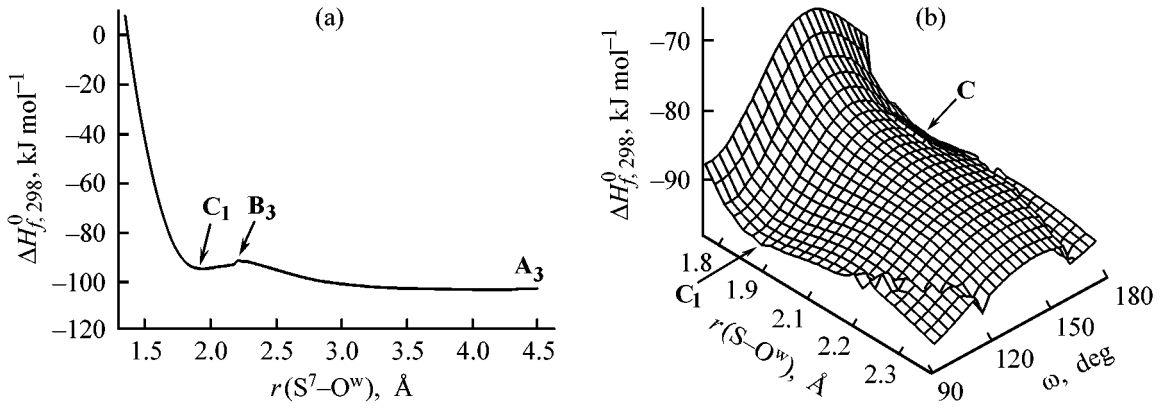

Fig. 4. (a) Potential curve and (b) potential energy surface fragment for hydrolysis involving the rear attack by the water molecule of the sulfur atom from the sulfonyl chloride group.

Table 1. Energy and structural characteristics[a] of the reactants, products, transition states, and intermediates in gas-phase hydrolysis of benzenesulfonyl chloride

Parameter	**A**	$\mathbf{B_1^{\neq}}$	$\mathbf{B_2^{\neq}}$	$\mathbf{B_3^{\neq}}$	**C**	$\mathbf{C_1}$	$\mathbf{D^{\neq}}$	**E**
$-E_{rel}$, eV	1.1119	0.1994	0.6302	0.7527	0.6806	0.8267	0.3109	2.0041
ν_i, cm^{-1}	–	101.5*i*	228.6*i*	245.2*i*	–	–	169.7*i*	–
$-\Delta H^0_{f,298}$, $kJ\,mol^{-1}$	422.8	334.8	376.3	388.2	381.2	395.3	345.5	508.9
H^0_{298}, $J\,mol^{-1}\,K^{-1}$	594.2	425.1	443.0	442.5	443.6	440.9	430.0	488.6
$C^0_{p,298}$, $J\,mol^{-1}\,K^{-1}$	184.0	175.3	181.3	180.3	186.2	184.0	173.3	192.1
$r(C^1–S^7)$	1.752	1.761	1.778	1.757	1.783	1.766	1.764	1.763
$r(S^7–Cl^8)$	2.108	2.281	2.111	2.138	2.129	2.155	2.432	4.407
$r(S^7=O^9)$	1.426	1.475	1.458	1.454	1.468	1.473	1.453	1.435
$r(S^7–O^w)$	–	1.975	2.162	2.207	1.948	1.935	1.865	1.699
$\omega(C^1S^7Cl^8)$	97.30	91.65	93.13	94.08	91.96	92.48	80.95	80.00
$\omega(C^1S^7O^w)$	–	99.50	166.94	88.54	172.97	91.33	142.09	99.61
$\omega(Cl^8S^7O^9)$	106.10	137.35	110.37	102.02	109.66	100.34	122.90	131.26
$\omega(O^9S^7O^{10})$	119.70	109.64	123.06	122.38	125.00	124.39	122.39	120.85
$\omega(HOH)^w$	107.70	115.04	112.69	111.63	113.97	113.34	117.52	–
τ^w	–	62.46	37.18	277.62	55.74	272.10	81.70	93.36
τ	89.80	134.28	90.06	85.27	89.62	85.76	113.76	114.85
$p(S^7–Cl^8)$	0.563	0.410	0.578	0.520	0.549	0.491	0.257	0.007
$p(S^7–O^w)$	0	0.172	0.086	0.087	0.154	0.180	0.292	0.632
$q(S^7)$	2.32	2.36	2.33	2.34	2.35	2.35	2.42	2.41
$q(Cl^8)$	–0.44	–0.57	–0.42	–0.50	–0.45	–0.53	–0.68	–0.21
$q(O)^b$	–0.80	–0.82	–0.82	–0.82	–0.83	–0.83	–0.85	–0.86
$q(O^w)$	–0.36	–0.47	–0.45	–0.46	–0.45	–0.46	–0.47	–0.67
$q(H^w)^b$	0.18	0.29	0.26	0.27	0.27	0.29	0.31	0.26
μ, D	–	5.80	2.35	6.09	1.53	7.09	3.16	4.13

[a] $E_{rel} = E + 2201$, where E is the total energy; ν_i are the imaginary vibrational frequencies for transition states; r are the interatomic distances, Å; ω and τ are the bond and torsion angles, deg; p are the bond orders; q are the atomic charges; and μ are the dipole moments. [b] The largest charges for two atoms.

the initial state **A** corresponding to isolated reactants to the state **E** corresponding to the reaction products. The first route (1a) corresponds to the frontal, and the second (1b), to the axial attack by the water molecule of the sulfur atom from the sulfonyl chloride group.

$$\underset{\mathbf{A}}{PhSO_2Cl} + H_2O \rightarrow \mathbf{B_1^{\neq}} \rightarrow \mathbf{C} \rightarrow \mathbf{D^{\neq}} \rightarrow \underset{\mathbf{E}}{PhSO_2OH} + HCl \quad (1a)$$

$$\underset{\mathbf{A}}{PhSO_2Cl} + H_2O \rightarrow \mathbf{B_2^{\neq}} \rightarrow \mathbf{C} \rightarrow \mathbf{D^{\neq}} \rightarrow \underset{\mathbf{E}}{PhSO_2OH} + HCl \quad (1b)$$

Both reaction pathways include two elementary stages of which the first involves formation of the intermediate complex **C** (five-coordinate intermediate) which is further converted to the reaction products via the transition state $\mathbf{D^{\neq}}$ in the second stage by the monomolecular mechanism.

Table 1 lists the total energies, as well as the thermodynamic parameters, the charge distribution data, the dipole moments, and the major structural parameters for the initial (**A**) and final (**E**) states, as well as for all the transition states and reaction intermediates revealed, namely, $\mathbf{B_1^{\neq}}$, $\mathbf{B_2^{\neq}}$, $\mathbf{B_3^{\neq}}$, **C**, $\mathbf{C_1}$, and $\mathbf{D^{\neq}}$. For the transition states, the imaginary vibrational frequencies ν_i are also presented.

We calculated for all the elementary stages of reaction pathways (1a) and (1b), as well as for the elementary stage $\mathbf{A} \rightarrow [\mathbf{B_3^{\neq}}] \rightarrow \mathbf{C_1}$, the activation parameters, the changes in the thermodynamic functions, and the rate constants (Table 2). The latter were calculated by the known Eyring equation [24]. The apparent values of the activation parameters,

Table 2. Activation parameters, rate constants,[a] and thermodynamic functions at 298 K for the elementary stages of gas-phase hydrolysis of benzenesulfonyl chloride

Parameter	Elementary stages of reaction			
	$\mathbf{A} \rightarrow [\mathbf{B_1^{\neq}}] \rightarrow \mathbf{C}$, frontal attack	$\mathbf{A} \rightarrow [\mathbf{B_2^{\neq}}] \rightarrow \mathbf{C}$, axial attack	$\mathbf{A} \rightarrow [\mathbf{B_3^{\neq}}] \rightarrow \mathbf{C_1}$, rear attack	$\mathbf{C} \rightarrow [\mathbf{D}^{\neq}] \rightarrow \mathbf{E}$
$\Delta H^{\neq}$, kJ mol^{-1}	88.0 (46.4)	46.5 (4.9)	34.7 (7.2)	35.7 (163.4)
$\Delta S^{\neq}$, J mol^{-1} K^{-1}	–169.1 (–18.4)	–151.3 (–0.6)	–151.7 (1.6)	–12.9 (–18.8)
$\Delta C_p^{\neq}$, J mol^{-1} K^{-1}	–8.7 (–10.9)	–2.7 (–4.9)	–3.7 (–3.8)	–13.6 (–58.7)
ln k	–26.4 (8.5)	–7.50 (27.4)	–2.79 (26.7)	13.5 (–43.5)
k, l mol^{-1} s^{-1}	3.50×10^{-12} (5049)	5.54×10^{-4} (8.0×10^{11})	0.061 (4.1×10^{11})	7.33×10^{5}[b] (1.3×10^{-19})
ΔH^0, kJ mol^{-1}	41.6		27.5	–127.7
ΔS^0, J mol^{-1} K^{-1}	–150.7		–153.3	45.1
$\Delta C_p^{\neq}$, J mol^{-1} K^{-1}	2.2		0.07	5.9
ΔG^0, kJ mol^{-1}	86.5		73.2	–141.1
ln K_e	–34.9		–29.5	56.9

[a] Given in parentheses are the corresponding parameters for reverse stages. [b] Monomolecular constant in s^{-1}.

namely, activation enthalpies and entropies for both routes (1a) and (1b), can be calculated as follows:

$$\Delta H^{\neq}_{\text{app, I}} = \Delta H^{\neq}_{1, \text{I}};\ \Delta S^{\neq}_{\text{app, I}} = \Delta S^{\neq}_{1, \text{I}}. \quad (2a)$$

$$\Delta H^{\neq}_{\text{app, II}} = \Delta H^{\neq}_{1, \text{I}} - \Delta H^{\neq}_{-1, \text{I}} + \Delta H^{\neq}_2 = \Delta H_1 + \Delta H^{\neq}_2;$$
$$\Delta S^{\neq}_{\text{app, II}} = \Delta S^{\neq}_{1, \text{I}} - \Delta S^{\neq}_{-1, \text{I}} + \Delta S^{\neq}_2 = \Delta S_1 + \Delta S^{\neq}_2. \quad (2b)$$

In expressions (2a) and (2b) the indices 1 and 2 designate the parameters corresponding to the first and second elementary stages, and indices I and II, to the frontal (1a) and axial (1b) routes of hydrolysis, respectively. The apparent rate constants can be calculated by substituting the apparent values of the activation parameters calculated by Eqs. (2a) and (2b) into Eq. (2). Table 3 lists the calculated apparent values of the activation parameters and rate constants for the both reaction routes, as well as the thermodynamic functions of the process.

Table 3. Calculated apparent values of the activation parameters and rate constants and thermodynamic functions of gas-phase hydrolysis of benzenesulfonyl chloride at 298 K

Parameter	Value
$\Delta H^{\neq}_{\text{app, I}}$ ($\Delta H^{\neq}_{\text{app, II}}$), kJ mol^{-1}	88.0 (77.3)
$\Delta S^{\neq}_{\text{app, I}}$ ($\Delta S^{\neq}_{\text{app, II}}$), J mol^{-1} K^{-1}	–169.1 (–163.6)
$\Delta G^{\neq}_{\text{app, I}}$ ($\Delta G^{\neq}_{\text{app, II}}$), kJ mol^{-1}	138.4 (126.1)
$k_{\text{app, I}}$ ($k_{\text{app, II}}$), l mol^{-1} s^{-1}	3.50×10^{-12} (5.07×10^{-10})
$\Delta H^0_{\text{react}}$, kJ mol^{-1}	–86.1
$\Delta S^0_{\text{react}}$, J mol^{-1} K^{-1}	–105.6
$\Delta C^0_{p, \text{react}}$, J mol^{-1} K^{-1}	8.1
$\Delta G^0_{\text{react}}$, kJ mol^{-1}	–54.6

Table 3 shows that the apparent rate constant of hydrolysis for route II [axial attack by scheme (1b)] is 145 times that for route I [frontal attack by scheme (1a)]. The enthaply barrier for reaction route II is by 10.7 kJ mol^{-1} larger and the entropy barrier, by 5.5 J mol^{-1} K^{-1} smaller than those for route I. This suggests that in the gas phase the hydrolysis follows predominantly route (1b) involving the axial attack by the water molecule of the sulfur atom from the sulfonyl chloride group. In what follows, route 1b will be taken as the principal route, which suggests $\Delta H^{\neq}_{\text{app}} = \Delta H^{\neq}_{\text{app, II}}$, $\Delta S^{\neq}_{\text{app}} = \Delta S^{\neq}_{\text{app, II}}$, $k_{\text{app}} = H_{\text{app, II}}$.

Thus, gas-phase hydrolysis of benzenesulfonyl chloride is a two-stage exothermic process whose kinetic scheme can be represented as

$$\underset{\mathbf{A}}{\text{PhSO}_2\text{Cl}} + \text{H}_2\text{O} \underset{k_{-1}}{\overset{k_1}{\rightleftarrows}} \mathbf{C} \xrightarrow{k_2} \underset{\mathbf{E}}{\text{PhSO}_2\text{OH}} + \text{HCl}. \quad (3)$$

In the first, equilibrium, stage, which is realized primarily by the axial attack of the sulfur atom by the water molecule, a five-coordinate intermediate **C** is formed via the transition state $\mathbf{B_2^{\neq}}$. In the second stage, this intermedaiate breaks down into hydrolysis products via the transition state $\mathbf{D}^{\neq}$. As follows from Table 2, the first, equilibrium, stage of hydrolysis involves heat absorption ($\Delta H^0_1 = 41.6$ kJ mol^{-1}) and is

Table 4. Apparent rate constants and activation parameters of hydrolysis of benzenesulfonyl chloride in the gas phase, water, and aqueous dioxane

Solvent	T, K	k_{app}, l mol^{-1} s^{-1}	$\Delta H^{\neq}_{app}$, kJ mol^{-1}	$\Delta S^{\neq}_{app}$, J mol^{-1} K^{-1}	References
Gas phase	298	5.10×10^{-10}	77.3	–163.6	[a]
Water–dioxane (x_2 0.954)	313	$(8.51 \pm 0.05) \times 10^{-8}$[b]	–	–	[4]
Water–dioxane (x_2 0.329)	303	$(5.24 \pm 0.06) \times 10^{-6}$[b]	52.8 ± 1.3	–171.9 ± 4.1[c]	[5]
Water	298	5.69×10^{-5}[b]	71.5 ± 1.9	–86.7 ± 6.4[c]	[7]
〃	298	5.51×10^{-5}[b]	68.6 ± 0.8	–96.7 ± 3.3[c]	[2]

[a] This work. [b] The values are obtained from the experimental pseudomonomolecular rate constants ($k_{app, mono}$) by the formula $k_{app} = K_{app, mono}/C_{H_2O}$. [c] The activation entropies were calculated by processing the temperature dependence of the bimolecular rate constants (in the cited works, the activation parameters were calculated from the temperature dependence of the pseudomonomolecular rate constants).

accompanied by a significant decrease in the entropy (ΔS^0_1 = –150.7 J mol^{-1} K^{-1}). This is manifested in a very small equilibrium constant of formation of adduct **C**, $K_1 = 7 \times 10^{-16}$. As K_1 is more than 20 orders of magnitude lower than the rate constant of the second stage k_2, the overall rate of the process is determined by K_1. Formation of complex **C** in the first stage should directly involve vacant 3*d* orbitals of the sulfur atom, as the S^7–O^w bond in the complex with the order of 0.15, most probably, has a covalent character (for comparison, the S–Cl and S–O bonds in the molecules of compound **II** and its hydrolysis product, benzenesulfonic acid, have orders of 0.56 and 0.63, respectively).

The data on the charge distribition for the $\mathbf{B}^{\neq}_1$ and $\mathbf{B}^{\neq}_2$ states (Table 1) suggest a greater polarity of the first transition state. The charges localized on the S and Cl atoms of the sulfo group, as well as on the H^w and O^w atoms in the transition state $\mathbf{B}^{\neq}_1$, exceed those in the $\mathbf{B}^{\neq}_2$ state. The difference in the charges is the greatest for the Cl atom. The $\mathbf{B}^{\neq}_1$ state has a more strained structure: It is characterized by greater S^7–Cl^8 and S^7=O^9 interatomic distances; the bond angle $Cl^8S^7O^9$ is markedly greater, and the bond angle $O^9S^7O^{10}$ is markedly smaller than in $\mathbf{B}^{\neq}_2$. The structure of the transition state $\mathbf{B}^{\neq}_2$ is much closer to that of complex **C** than of the reactants. All the transition states of the reaction are strongly asymmetric.

In the second stage of the reaction, as the system passes through the transition state $\mathbf{D}^{\neq}$, a chlorine atom is eliminated from the sulfur atom of the sulfo group and a proton, from the oxygen atom of water, forming a neutral HCl molecule. The water molecule changes its axial position to the equatorial position, which requires a decrease in the $C^1S^7O^w$ angle from 173° to 100°. Elimination of the chlorine atom is accompanied by strengthening of the S^7–Cl^8 bond polarization and, consequently, by growth of the charges on the S and Cl atoms. Judging from the charge distribution pattern, the $\mathbf{D}^{\neq}$ state is much more polar than all the other reaction states. Polar media will, evidently, facilitate elimination of the chlorine atom and favor a decrease in the contribution from $\Delta H^{\neq}_2$ to the apparent activation enthalpy.

Table 4 compares the h_{app}, $\Delta H^{\neq}_{app}$, and $\Delta S^{\neq}_{app}$ values calculated in this work with the published experimental data on hydrolysis of **II** in water [2, 7] and aqueous-dioxane solvent of different compositions [4, 5]. As seen from Table 4, h_{app} in the gas phase proved to be two orders of magnitude smaller than in the case of hydrolysis in a highly concentrated aqueous-dioxane solvent (x_2 = 0.954) whose low polarity (ε ~2) makes it the reaction medium closest to the gas phase. The calculated activation entropy is consistent with the trend observed for aqueous dioxane, namely, that with decreasing water content in an aqueous-organic solvent $\Delta S^{\neq}_{app}$ tends to sharply decrease (growth of the entropy barrier). Indeed, the calculated $\Delta S^{\neq}_{app}$ value for the gas phase proves to be very close to that for hydrolysis in 70% (by mass, x_2 = 0.392) aqueous dioxane. The enthalpy barrier for the reaction in the gas phase is by 24 kJ mol^{-1} higher than for hydrolysis in 70% aqueous dioxane and by 9 kJ mol^{-1} higher than for hydrolysis in water.

Formation of the **C** type five-coordinate intermediates in hydrolysis and other nucleophilic processes involving arylsulfonyl halides was presumed earlier [10, 11]. It was believed that such intermediates can form in hydrolysis in weakly polar media, e.g., in concentrated aqueous dioxane solutions, where solvation of the leaving halide ion is hindered. These conditions favor the two-stage addition–elimination

mechanism S_AN [scheme (4)] involving formation of the metastable five-coordinate intermediate with a negative charge localized on the sulfonyl oxygen in the first stage. In the second, limiting, stage, the leaving group is eliminated from the intermediate.

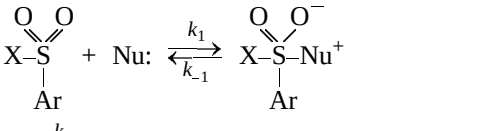

(4)

The kinetic experiment does not allow deciding between the S_N2 and S_AN mechanisms in view of the lack of experimental evidence of the existence of five-coordinate intermediates shown in scheme (4). As to hydrolysis of compounds **I** in more polar media such as, e.g., water and dilute aqueous dioxane solutions, the authors of [8, 10, 11] give preference to the single-stage asynchronous S_N2 process passing, according to scheme (5), through a trigonal-bipyramidal transition state.

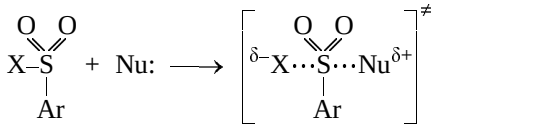

(5)

Our calculations support the assumed existence of five-coordinate intermediates in the hydrolysis pathway for compounds **I** and, thus, can speak in favor of the S_AN hydrolysis route in weakly polar media. These calculations also support the assumption made in [11] that the intermediate in scheme (4) is extremely unstable and is characterized by a "fairly shallow well in the reaction pathway." In this case, according to the Hammond's postulate, the transition states for each stage of the two-stage process (4) are structurally close to the intermediate product. As seen from Table 1 and Fig. 3, the structure of the transition states $\mathbf{B}_2^{\neq}$ and $\mathbf{D}^{\neq}$ is actually close to that of intermediate **C**.

Although the kinetic schemes (3) and (4) for the two-stage mechanism of hydrolysis of compounds **I** based on the results of our quantum-chemical calculations are very close to those proposed in [10, 11], our results lead to somewhat different conclusions concerning the limiting stage of the process and the charge distribution pattern for the intermediate formed. First, the calculation shows that the second stage is not a limiting stage, as k_{app} is determined primarily by the equilibrium constant K_1 of the first stage of hydrolysis: $k_{app} = K_1k_2$, with $K_1 = 7 \times 10^{16}$ and $k_2 = 7.33 \times 10^5$ (comparison of the rates of the forward reactions shows that the first stage should be the limiting stage, as $k_1 << k_2$). As to the apparent activation enthalpy $\Delta H_{app}^{\neq}$ defined by formula (2b) as the sum of the enthalpy of the first stage ΔH_1 and the activation enthalpy of the second stage of the reaction $\Delta H_2^{\neq}$, the contributions from these two parameters to the apparent enthaply proved to be comparable (41.6 and 35.7 kJ mol^{-1}, respectively). Second, according to the charge distribution pattern (Table 1), the negative charge in the intermediate **C** is not localized on the oxygen atom from the sulfonyl group. Compared to the initial state of the reaction, there is a certain growth of the negative charge on the O^w atom (by 25%) and of the positive charge on the H^w atoms (by 50%) of the water molecule, while the sulfur, chlorine, and oxygen atoms of the sulfonyl chloride group do not exhibit significant changes in the electron density distribution pattern. Lastly, the structural models for the transition state proposed in [10, 11] for the bimolecular mechanism S_N2 [scheme (5)] and five-coordinate intermediate for the two-stage mechanism S_AN [scheme (4)] imply, essentially, a rear attack by the nucleophile, while our calculations suggest the predominantly axial orientation of the attack. It should be taken into account, however, that the conclusions made in this work hold for the gas-phase process. At the same time, the previously proposed mechanisms of hydrolysis of compounds **I** and the structural models of the transition states are based on the kinetic data obtained for polar aqueous-organic solvents, where the structural effects and specific solvation are of great importance. The influence of the hydration effects on the mechanism of the elementary stages of benzenesulfonyl chloride hydrolysis will be discussed in subsequent works.

ACKNOWLEDGMENTS

This work was financially supported by the International Soros Program of Education in the Field of Exact Sciences (grant no. 573d).

REFERENCES

1. Rogne, O., *J. Chem. Soc. B.*, 1968, pp. 1294–1296; Robertson, R.E. and Rossal, B., *Can. J. Chem.*, 1971, vol. 49, pp. 1441–1450; Robertson, R.E. and Rossal, B., *Can. J. Chem.*, 1971, vol. 49, pp. 1451–1455; Haughton, A.R., Laird, R.M., and Spence, M.J., *J. Chem. Soc., Perkin Trans. 2*, 1975, no. 6, pp. 637–643.
2. Rogne, O., *J. Chem. Soc., B*, 1970, pp. 1056–1058.
3. Vizgert, R.V., *Usp. Khim.*, 1963, vol. 32, no. 1, pp. 3–39; Vizgert, R.V., Rubleva, L.I., and Maksi-

menko, N.N., *Zh. Org. Khim.*, 1990, vol. 26, no. 12, pp. 2605–2609; Rubleva, L.I., Maksimenko, N.N., and Vizgert, R.V., *Kinet. Katal.*, 1992, vol. 33, no. 1, pp. 43–48.

4. Rubleva, L.I., Maksimenko, N.N., and Vizgert, R.V., *Kinet. Katal.*, 1992, vol. 33, no. 4, pp. 760–764.
5. Vizgert, R.V., Rubleva. L.I., and Maksimenko, N.N., *Zh. Org. Khim.*, 1989, vol. 25, no. 4, pp. 810–814.
6. Gnedin, V.G., Ivanov, S.N., and Shchukina, M.V., *Zh. Org. Khim.*, 1988, vol. 24, no. 4, pp. 810–817; Kislov, V.V., Ivanov, S.N., and Gnedin, B.G., *Zh. Org. Khim.*, 1996, vol. 32, no. 5, pp. 716–721; Kislov, V.V., Ivanov, S.N., and Noskov, S.Yu., *Zh. Obshch. Khim.*, 1997, vol. 67, no. 8, pp. 1330–1336; Kislov, V.V., Ivanov, S.N., and Gnedin, B.G., *Zh. Obshch. Khim.*, 1999. vol. 69, no. 3, pp. 479–487.
7. Ivanov, S.N., Gnedin, B.G., and Shchukina, M.V., *Zh. Org. Khim.*, 1990, vol. 26, no. 7, pp. 1415–1422; Gnedin, B.G., Ivanov, S.N., and Spryskov, A.A., *Zh. Org. Khim.*, 1976. vol. 12, no. 9, pp. 1939–1943.
8. Arcoria, A., Ballisteri, F.R., Musumarra, G., and Tomaselli, G.A., *J. Chem. Soc., Perkin Trans. 2*, 1981, no. 2, pp. 221–227; Ballisteri, F.P., Cantone, A., Maccarone, E., Tomaselli, G.A., and Tripolone, M., *J. Chem. Soc., Perkin Trans. 2*, 1988, no. 4, pp. 438–441; Arcoria, A., Ballisteri, F.P., Spina, E., Tomaselli, G.A., and Maccarone, E., *J. Chem. Soc., Perkin Trans. 2*, 1988, no. 10, pp. 1793–1798; Ballisteri, F.P. and Tomaselli, G.A., *J. Heterocyclic Chem.*, 1981, vol. 18, no. 6, pp. 1229–1234.
9. Kice, J., *Adv. Phys. Org. Chem.*, 1980, vol. 17, pp. 65–181.
10. Vizgert, R.V., Skrypnik, Yu.G., Starodubtseva, M.P., Maksimenko, N.N., and Sheiko, S.G., Available from VINITI, no. 1237–76; *Ref. Zh. Khim.*, 1976, 16Zh47Dep.
11. Litvinenko, L.M., Savelova, V.A., Solomoichenko, T.N., and Zaslavskii, V.G., in *Struktura, reaktsionnaya sposobnost' organicheskikh soedinenii i mekhanizmy reaktsii* (Structure, Reactivity of Organic Compounds, and Reaction Mechanisms), Kiev: Naukova Dumka, 1980, pp. 3–68.
12. Bazilevskii, M.V., Koldobskii, S.G., and Tikhomirov, V.A., *Usp. Khim.*, 1986, vol. 55, no. 10, pp. 1667–1698.
13. Bazilevskii, M.V., Koldobskii, S.G., and Tikhomirov, V.A., *Zh. Org. Khim.*, 1984, vol. 20, no. 5, pp. 908–913.
14. Jorgensen, W.L. and Buckner, J.K., *J. Phys. Chem.*, 1986, vol. 90, no. 19, pp. 4651–4654.
15. Burshtein, K.Ya. and Isaev, A.N., *Zh. Strukt. Khim.*, 1985, vol. 26, no. 3, pp. 16–20; Burshtein, K.Ya. and Isaev, A.N., *Izv. Akad. Nauk SSSR, Ser. Khim.*, 1985, no. 5, pp. 1066–1070.
16. Petrov, V.M., Petrova, V.N., Kislov, V.V., Ivanov, S.N., Girichev, G.V., Noskov, S.Yu., and Krasnov, A.V., *Zh. Strukt. Khim.*, 1999, vol. 40, no. 4, pp. 653–664.
17. Kislov, V.V., Petrov, V.M., Noskov, S.V., Petrova, V.N., and Ivanov, S.N., *Internet J. Chem.*, 1999, vol. 2, article 9.
18. Kislov, V.V. and Ivanov, S.N., *Zh. Obshch. Khim.*, 2000, vol. 70, no. 2, pp. 208–216.
19. Zhidomirov, G.M., Bagatur'yants, A.A., and Abronin, I.A., *Prikladnaya kvantovaya khimiya. Raschety reaktsionnoi sposobnosti i mekhanizmov khimicheskikh reaktsii* (Applied Quantum Chemistry. Calculations of the Reactivity and Mechanisms of Chemical Reactions), Moscow: Khimiya, 1979.
20. Minkin, V.I., Simkin, B.Ya., and Minyaev, R.M., *Kvantovaya khimiya organicheskikh soedinenii. Mekhanizmy reaktsii* (Quantum Chemistry of Organic Compounds. Reaction Mechanisms), Moscow: Khimiya, 1986.
21. Stewart, J.J.P., *J. Comput. Chem.*, 1989, vol. 10, pp. 209–220.
22. Stewart, J.J.P., *J. Computer-Aided Mol. Des.*, 1990, no. 4, pp. 1–105; Stewart, J.J.P., *Mopac Manual*, US: Air Force Academy, Frank J. Seiler Research Laboratory, 1990, no. CO 80840.
23. Voityk, A.A. and Bliznyuk, A.A., *Zh. Strukt. Khim.*, 1992, vol. 33, no. 6, pp. 157–183.
24. Glasstone, S., Laidler, K.J., and Eyring, H., *The Theory of Rate Processes. The Kinetic of Chemical Reactions, Viscosity, Diffusion, and Electrochemical Phenomena*, New York, 1941.